

# Development of a digital video-microscopy technique to study lactose crystallisation kinetics in situ

María Paz Arellano, José Miguel Aguilera and Pedro Bouchon\*

*Departamento de Ingeniería Química y Bioprocesos, Escuela de Ingeniería, Pontificia Universidad Católica de Chile, Santiago, Chile*

Received 1 July 2004; received in revised form 15 September 2004; accepted 15 September 2004

Available online 18 October 2004

**Abstract**—Polarised light microscopy was employed non-invasively to monitor lactose crystallisation from non-seeded supersaturated solutions in real time. Images were continuously recorded, processed and characterised by image analysis, and the results were compared with those obtained by refractometry. Three crystallisation temperatures (10, 20 and 30 °C) and three different levels of initial relative supersaturation ( $C/C_s = 1.95; 2.34; 3.15$ ) were investigated. Induction times using the imaging technique proved to be substantially lower than those determined using refractive index. Lactose crystals were isolated digitally to determine geometrical parameters of interest, such as perimeter, diameter, area, roundness and Feret mean, and to derive crystal growth rates. Mean growth rates obtained for single crystals were fitted to a combined mass transfer model ( $R^2 = 0.9766$ ). The model allowed the effects of temperature and supersaturation on crystallisation rate to be clearly identified. It also suggested that, in this set of experiments, surface integration seemed to be the rate controlling step. It is believed that a similar experimental set-up could be implemented in a real food system to characterise a particular process where crystallisation control is of interest and where traditional techniques are difficult to implement.

© 2004 Elsevier Ltd. All rights reserved.

**Keywords:** Video microscopy; Image analysis; Lactose crystallisation; Food microstructure

## 1. Introduction

In some food products (such as sweetened condensed milk, ice cream or chocolate) quality is highly dependent on crystallisation control during processing and storage. In these foods, a small variation in certain external conditions can lead to unwanted changes (graininess or bloom) with negative consequences on their quality and acceptability. Consequently, knowledge on how and why crystals form in those foods is crucial to produce consistent and high-quality products.<sup>1</sup>

The main sugar in milk is lactose, representing between 4% and 6% of milk total solids.<sup>2</sup> Therefore, a deep understanding of its crystallisation behaviour is often needed in dairy products manufacturing. In addition,

$\alpha$ -lactose monohydrate is produced industrially in considerable amounts, finding use in a wide range of products in the food industry.<sup>3</sup>

Several studies on lactose crystallisation kinetics have been carried out through the years. Polarimetry, refractometry and gravimetric methods have been extensively used to characterise lactose crystallisation kinetics.<sup>4–8</sup> Growth kinetics of crystal aggregates in stagnant solutions and seed crystals in agitated solutions have been determined using those methods. In addition, the influences of temperature and supersaturation on crystallisation, as well as other factors such as the presence of additives or impurities, agitation rates and seed surface area have been investigated. Many of these studies have been particularly focused on lactose crystallisation in milk whey systems, an issue of major concern to the dairy industry, because whey is the principal source for lactose production. Evidently, the experimental work has included most of the impurities commonly

\* Corresponding author. Tel.: +56 2 3547962; fax: +56 2 3545803; e-mail: [pbouchon@ing.puc.cl](mailto:pbouchon@ing.puc.cl)

present in whey systems, while on the contrary, research on pure lactose containing systems has been less reported.<sup>9</sup>

Over the past decades, the study of crystallisation kinetics using photographic and microphotographic techniques has gained much attention because it allows both documentation of the nature of the growing crystals and provides quantitative information about geometrical features of interest. In fact, as pointed out by Stanley et al. and Aguilera and Stanley, today microscopy is probably the most widely used technique for characterising structure in foods, especially those with crystalline content.<sup>10,11</sup> One of the pioneering works on lactose crystallisation was carried out by Van Kreveland and Michaels, based on the procedure developed by Kucharenko.<sup>6,12,13</sup> In their experiments, they grew lactose crystals individually in a rotating flask and took microphotographs of the single crystals over time. Subsequently, they analysed the changes in facial areas using tracing paper and determined the growth rates of various faces of well-developed tomahawk-shaped  $\alpha$ -lactose. The lack of an accurate instrument to measure small changes occurring during growth led Valle-Vega and Nickerson to develop a procedure using an image analyser computer to measure the changes in the distribution of crystal area during crystal growth in seeded and agitated lactose solutions.<sup>6</sup>

Recently, new methods for food quality characterisation have been developed. Among these techniques, video-microscopy and image analysis methods have been increasingly used to understand and quantify dynamic changes occurring at the microstructural level. Two important advantages of these methods are (1) they minimise the artefacts introduced by other techniques and (2) the observation can be continuously recorded in situ. The latter advantage is complementary with the concept of miniaturisation of experiments coined by Aguilera and Lillford, which refers to the transfer of a real experiment to a thermally-controlled stage under the lens of a microscope, allowing temperature ramps and stationary periods to be programmed.<sup>14</sup> The system consists of a digital or video camera attached to a microscope that captures images in real time, which are instantaneously recorded in a personal computer and subsequently analysed with appropriate image analysis software.<sup>15</sup> Following this approach, Shi et al. studied contact nucleation phenomena, that is, nucleation from a parent crystal, using a photomicroscopic cell.<sup>16</sup> In their set of experiments they were able to determine among other parameters, the growth rates for individual crystals taking into account the influence of neighbouring crystals.

The various imaging techniques developed until now had led researchers to several conclusions. Amongst them, is that all crystal habits of  $\alpha$ -lactose are crystallographically equivalent to the tomahawk form, which is the result of the dissimilar relative growth rates of the different faces. Tomahawk-shaped crystals grow mainly

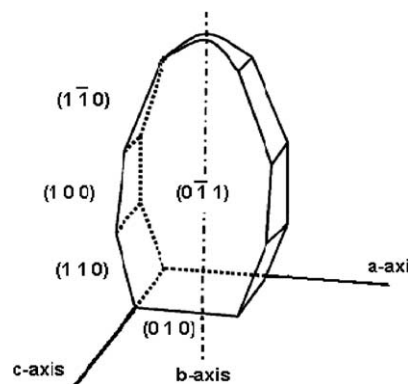


**Figure 1.** Tomahawk-shaped  $\alpha$ -lactose crystal. Faces are indicated by their Miller index (from Raghavan et al.).<sup>3</sup>

in one direction, that is, from the apex along the  $b$ -axis as shown in Figure 1.<sup>1,12</sup> Another important conclusion is in relation to the growth rates of individual faces and their projected areas, which have shown to be linear during the initial stages.<sup>12,16,17</sup>

Also, it has been reported that crystals of uniform shape and size growing under the same environmental conditions do not grow at the same rate.<sup>1</sup> This phenomenon is known as growth rate dispersion (GRD) and has been modelled for lactose secondary nucleation.<sup>12</sup> GRD has a great impact on batch and continuous sugar production systems and continuous research is being carried out on this topic.<sup>18</sup>

The great potential of modern video-microscopy and image analysis techniques is evident and is being discovered by food researchers. As a matter of fact, several studies have made use of this technique during the last decade to quantify microstructural changes during heating, frying and crystallisation, among other unit operations.<sup>15,19–24</sup> In relation to lactose crystallisation, microimaging techniques have only been used to assess lactose crystallisation in seeded crystal solutions. However, there is a lack of information in relation to spontaneous lactose crystallisation using this technique. We believe that the development of a procedure that allows the study of spontaneous lactose crystallisation under the lens of a microscope in real time is of great interest because high-resolution digital imaging nowadays permits precise quantification of phenomena. In addition, it is believed that such a procedure could be relatively easily adapted to study fluid food systems that exhibit spontaneous crystallisation.

The main objectives of this work were to develop a non-invasive method to monitor lactose crystallisation from non-seeded supersaturated solutions, considering the influence of growing neighbouring crystals and to implement an image analysis procedure to characterise crystal growth patterns to derive associated crystallisation rates.

## 2. Results and discussion

### 2.1. Crystallisation kinetics: digital imaging versus refractometry

When studying crystallisation based on spontaneous nucleation, the lag time required for the first detectable evidence of nuclei formation becomes a relevant parameter. The induction time in a crystallisation process is composed of the true time required for nuclei to form, plus the time required for a nucleus to grow to a detectable size. Thus, the induction time depends to a large extent on the sensitivity of the detection technique.<sup>1</sup>

Overall, digital imaging and refractometry show a decrease in induction time with increasing supersaturation and/or temperature, under these experimental conditions. Previous investigations on crystallisation of various substances at temperatures higher than 0°C in non-viscous systems have shown the same effects on induction time.<sup>1</sup> However, measurements using refractive index yielded considerably longer induction times than those determined using the digital imaging technique. As can be seen in Figures 2 and 3, small nuclei could be detected at early stages using microscopy. However, as shown in Figure 4, it was not until many crystals formed and started to grow that a noticeable change in refractive index and, therefore, in solution concentration could be detected. For instance, changes in refractive index at a relative supersaturation of 2.34 and a crystallisation temperature of 10°C were not even detected after 96 h. On the other hand, induction times using the imaging technique were much shorter because it was possible to detect crystals as small as 4 µm. In fact,

all the experiments carried out at 20 and 30°C and the experiments that were carried out at 10°C with a relative supersaturation of 3.15 gave induction times of less than 2 h using the imaging technique. From these results it is clear that refractive index measurement is not a sensitive enough technique to assess crystallisation at early stages and should only be used when massive crystallisation occurs. In contrast, digital microscopy is instrumental at early crystallisation times but loses its sensitiveness at longer times when overlapping of crystals occurs. In food systems where crystallisation may be a defect (e.g., lactose in dairy products such as ice cream or caramel spread), a clear identification of the induction time needs to be carried out. Because digital microscopy gives a good idea of the time required to initiate crystallisation, the development of a similar technique based on image analysis should certainly give useful information on specific food products.

The effects of supersaturation and temperature on crystallisation rate were well detected at shorter times by digital microscopy. In our set of experiments this is reflected by the steeper increase in total area occupied by crystals, which is observed at higher supersaturations and at higher temperatures, maintaining all other parameters constant (Fig. 3). The same effects were observed when using refractometry for extended experimental times (up to 96 h). When constant supersaturation was maintained, crystallisation rates were higher with increasing temperature because of the promoting effect of higher temperatures on nucleation rates and mass transfer steps, as explained by Jelen and Coulter.<sup>25</sup> The same effect of temperature was found by Thurby when studying  $\alpha$ -lactose crystallisation kinetics.<sup>26</sup> Also,

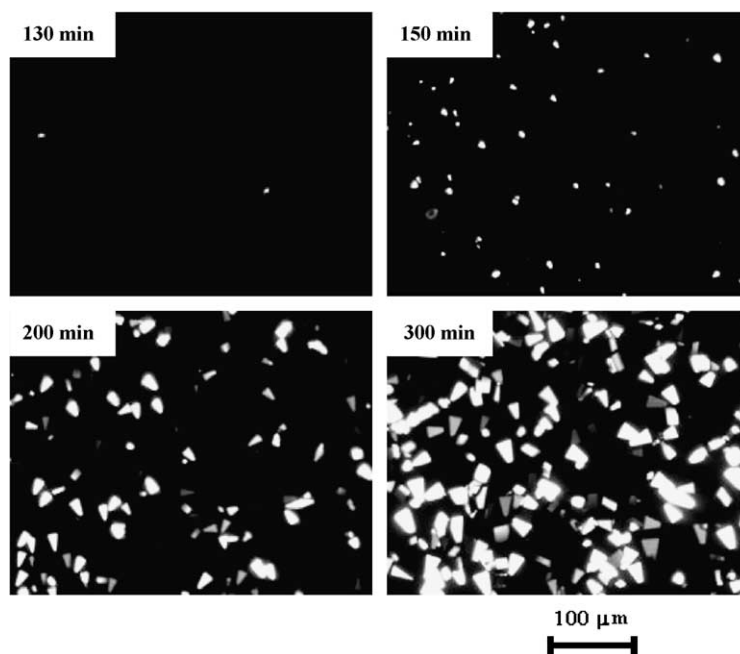
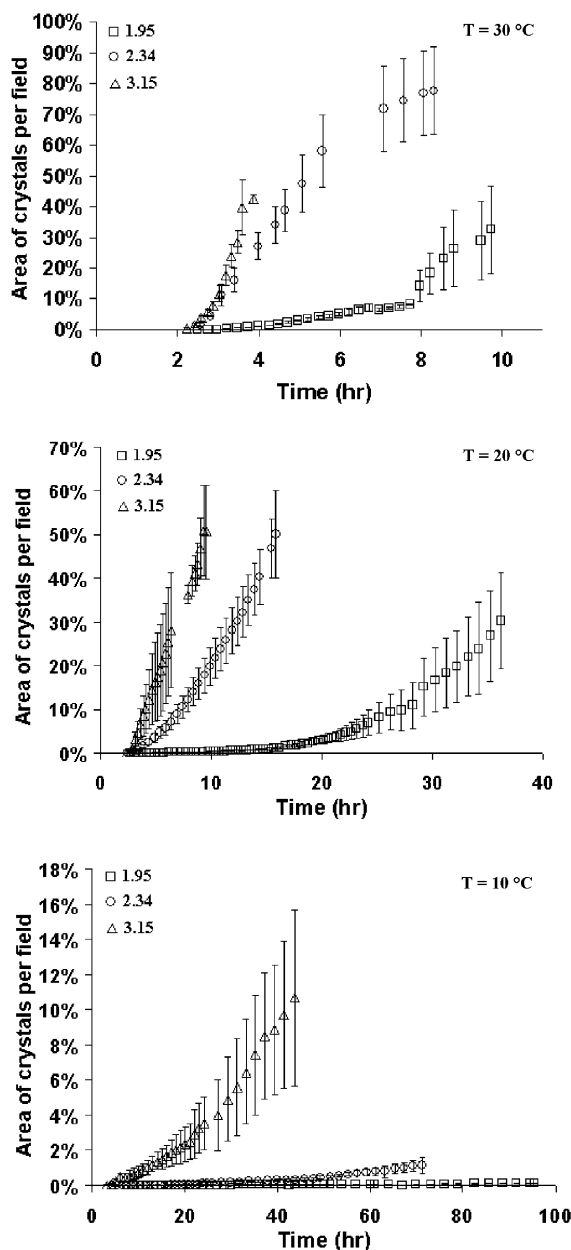


Figure 2. Sequence of images of  $\alpha$ -lactose crystals during crystallisation at 30°C with an initial supersaturation of 2.34.



**Figure 3.** Crystallisation kinetics determined by digital imaging based on the count of total area of crystals per microscopic field. Values are mean  $\pm$  standard error.

higher supersaturations were found to increase the crystallisation rate when working at a fixed temperature in accordance with previously reported results.<sup>5,7,12,16,25,27</sup> It is worth remembering that the increase in crystallisation rate may be reversed when working with extremely high supersaturation and/or temperatures, due to a potential reduction in molecular mobility.<sup>1</sup>

In general, deviations in the amount of crystallised lactose were obtained between the replicates with both techniques. However, greater deviations were observed when using digital microscopy due to the differences in nucleation patterns (number of nuclei) that were observed in almost every run for each experimental

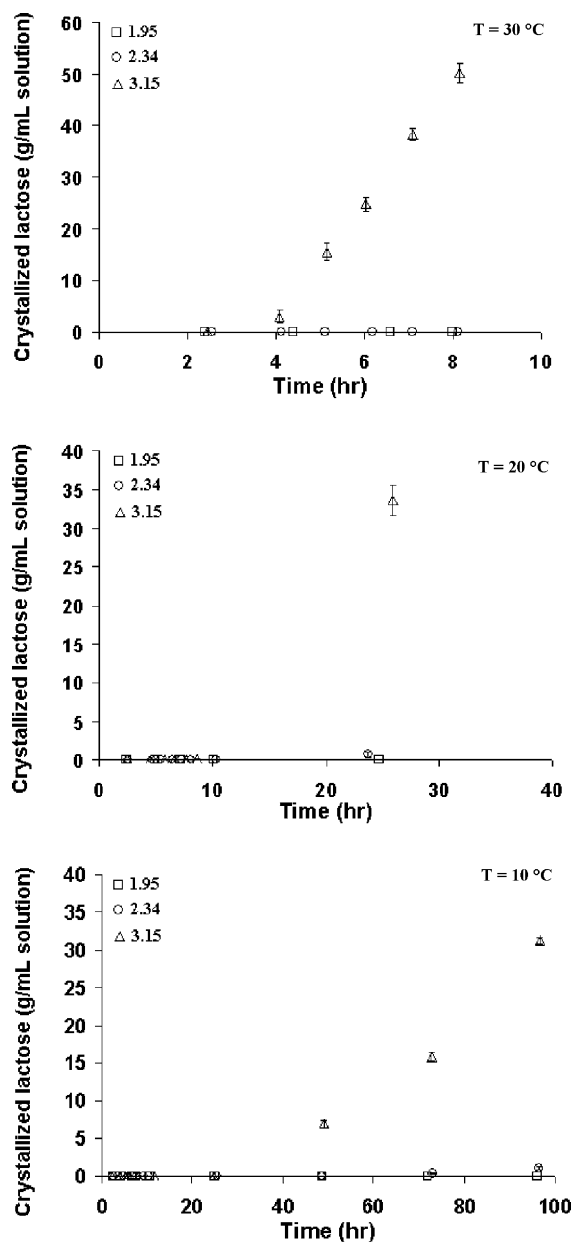


**Figure 4.** Crystallisation kinetics determined by refractometry. Values are mean  $\pm$  standard error.

set-up. As refractometry is a less sensitive technique, smaller changes were observed in each run, giving lower standard deviations. Garnier et al. have also detected highly fluctuating nucleation patterns with  $\alpha$ -lactose.<sup>27</sup> These differences are thought to be mainly because of the presence of impurities from lactose and/or water, which affect both nucleation and the crystal growth process.<sup>28</sup>

## 2.2. Single crystal analysis

Lactose crystals have several well-defined faces to lie upon when they are at the bottom of a sample holder

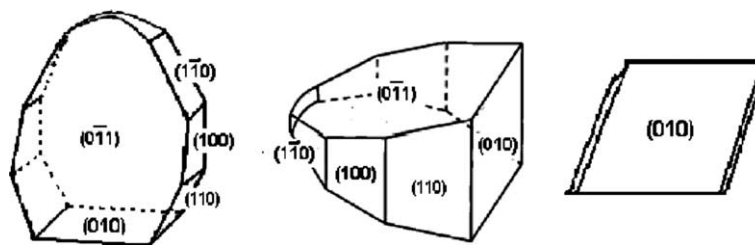


Figure 5.  $\alpha$ -Lactose tomahawk-shaped crystal seen from several perspectives (from Shi et al. and Raghavan et al.).<sup>3,16</sup>

(see Fig. 5). As reported by Shi et al. and Raghavan et al., most of the crystals lie either on their (100) face or on their (011) face.<sup>3,16</sup> Visual inspection of lactose crystals proved that two different shapes of crystals were present in the different experimental set-ups. Plate-shaped crystals lying on their (100) face cohabited with typical tomahawk-shaped crystals lying mostly on their (011) face. Plate-shaped crystals derive from the extremely slow growth of (011) and (010) faces in an otherwise tomahawk-shaped crystal, which is a consequence of a very slow growth along the  $a$ -axis direction (see Fig. 1).<sup>12</sup> At a supersaturation of 3.15, tomahawk-shaped crystals were observed to lie on their (010) face as well.

The existence of two different shapes of crystals within the same solution could be a consequence of the incorporation of different amounts or different kinds of impurities into the crystal lattice, because it has been proven that impurities can induce morphologic variations in lactose crystals by inhibiting the growth rate of certain faces.<sup>3,27,28</sup> The ratio of tomahawk to plate crystals increased when working at the highest supersaturation ( $C/C_s = 3.15$ ), supporting the hypothesis that impurities may be responsible for the formation of plate-shaped crystals by slowing the growth rate of the (011) face. In fact, several studies have recently revealed that impurities have a decreasing influence with increasing supersaturation as pointed out by Garnier et al.<sup>27</sup> Some of the different crystal shapes that were seen are shown in Figure 6.

As most of the crystals were lying on their (100) face, what was actually seen in the images of digitally isolated crystals was the projected image of faces (110), (100) and (1 $\bar{1}$ 0). It was impossible to distinguish the (110),

(100) and (1 $\bar{1}$ 0) faces of a plate crystal from the same faces of a tomahawk crystal without manually turning over the crystals, and therefore contaminating the sample solution. Only the (011) face was distinctly different between plate and tomahawk-shaped crystals (see Fig. 6) as noticed earlier by Van Kreveld and Michaels.<sup>12</sup>

Because of the inherent growth rate of the different faces of the crystal, the same projected faces were always selected when analysing single crystals. We chose the projected image of faces (110), (100) and (1 $\bar{1}$ 0), as it was clearly present in both tomahawk- and plate-shaped crystals, and this was the most common position that crystals adopted in all experimental conditions. As in previous imaging studies, the equivalent circular diameter was chosen as the characteristic size of the crystal.<sup>16</sup> The equivalent diameter corresponds to the diameter of a circle that has the same area as the particle.

To calculate the growth rate of a single crystal, an empirical linear fitting of the data, equivalent diameter versus time, was carried out. The assumption of linear behaviour of this characteristic size during initial lactose crystallisation has been adopted by several authors.<sup>12,16,25</sup> Approximately nine crystals per replicate were analysed; therefore each of the mean values presented in Table 1 corresponds to the average of approximately 27 crystals per experimental condition. ANOVA analysis of results showed no significant influence of replicates on growth rates at 95% confidence.

Due to the existence of growth rate dispersion, the mean growth rate values were used in the kinetic



Figure 6. Grey scale images of crystal shapes obtained in the different experiments. Projected images of (a) faces (110), (100) and (1 $\bar{1}$ 0) at supersaturations of 1.95 and 2.34, (b) faces (110), (100) and (1 $\bar{1}$ 0) at a supersaturation of 3.15, (c) face (011) of a plate-shaped crystal, (d) face (011) of a tomahawk crystal and (e) face (010).

Table 1. Calculated growth rates derived from the equivalent circular diameter increase of single crystals (data are means  $\pm$  standard error)

Relative supersaturation ( $C/C_s$ )	Initial lactose concentration (g/100 g water)	Temperature ( $^{\circ}\text{C}$ )	Growth rate ( $\mu\text{m/h}$ )	Mean $R^2$
1.95	27.6	10	$0.3 \pm 0.1$	0.943
1.95	37.2	20	$2.1 \pm 0.2$	0.980
1.95	50.0	30	$7.1 \pm 0.5$	0.988
2.34	33.2	10	$0.8 \pm 0.1$	0.975
2.34	44.6	20	$4.1 \pm 0.2$	0.982
2.34	60.0	30	$9.8 \pm 0.5$	0.973
3.15	44.7	10	$2.6 \pm 0.1$	0.977
3.15	60.0	20	$8.8 \pm 0.6$	0.973
3.15	80.8	30	$25.8 \pm 1.6$	0.975



analysis.<sup>16</sup> Mean growth rate values were fitted into a combined mass transfer model (Eq. 1), considering  $C/C_s - 1$  as the driving force for crystal growth.<sup>1,16</sup> This empirical model has been widely used before to fit crystallisation kinetic data at different supersaturation levels.<sup>1</sup>

$$Y = k * (S - 1)^n \quad (1)$$

where  $Y$  stands for the mean growth rate,  $k$  is a combined rate constant,  $n$  is a combined growth order and  $S = C/C_s$ .

Because the early stages of crystallisation were analysed, the value of  $C$  was assumed to remain constant and equal to the initial supersaturation for each experimental condition. This is a valid assumption at short times because initial crystallisation does not affect significantly solution concentration. This consideration is in agreement with refractometry measurements, which failed to detect changes in lactose concentration at early stages. To further confirm this criterion, an estimation of the weight of crystallised lactose in a sample holder was carried out. To do this, the mean weight of a crystal was derived from its surface area using the expression developed by Kucharenko for well-developed lactose crystals.<sup>6,13</sup> The expression relates the crystal surface to the crystal weight by  $A^3 = K * W^2$ , where  $A$  is the superficial area of all faces ( $\text{cm}^2$ ),  $W$  is the weight of the crystal (g) and  $K$  is an experimental constant, equal to  $115 \text{ cm}^6/\text{g}^2$ . The calculated weight was then multiplied by the number of crystals present in the holder, estimated from the count of crystals per visual field. Results demonstrated a decrease in the driving force of less than 1% in the most unfavourable case. Visser and Shi et al. also neglected changes in solution concentration in the early stages.<sup>16,17</sup>

The growth rate constant  $k$  in Eq. 2 was assumed to be related to temperature through the Arrhenius' equation:

$$k = k_0 * \exp\left(-\frac{E}{R * T}\right) \quad (2)$$

Replacement of this expression in Eq. 1 gave the following expression for the growth kinetic model:

$$Y = k_0 * \exp\left(-\frac{E}{R * T}\right) (S - 1)^n \quad (3)$$

Eq. 3 was linearised by applying a logarithmic function, obtaining Eq. 4:

$$\ln Y = \ln(k_0) - \frac{E}{R * T} + n \ln(S - 1) \quad (4)$$

The parameters  $\ln(k_0)$ ,  $E/R$  and  $n$  in Eq. 4 were obtained by linear regression using S-PLUS 6.1 software (Insightful Corporation, Seattle, USA) giving the following equation:

$$Y = 1.5 * 10^{17} * \exp\left(\frac{-22.7}{R * T}\right) * (S - 1)^2 \quad (5)$$

Collected data were adequately fitted by the combined model ( $R^2 = 0.9766$ ) and all parameters had a significant effect. Predicted curves (Eq. 4) and experimental results are plotted in Figure 7.

The value of the exponent  $n$  is related to the crystal growth mechanism or limiting step of the process. When diffusion from bulk solution to crystal surface is the limiting step,  $n$  is expected to be equal to unity. Higher orders point towards surface integration as the rate controlling step.<sup>1</sup> Several authors have found an exponent of the supersaturation term greater than unity when studying lactose crystallisation.<sup>5,12,16,25,26</sup> Reported values of  $n$  have ranged between 2 and 4, depending on the working temperature (from 0.5 to 70 °C), type of seed (single crystal or group of crystals) and measuring technique (gravimetric or polarimetric). The values of  $n$  obtained here cannot be compared with those previously reported because no values of  $n$  for spontaneous lactose crystallisation could be found in the literature. The estimated value of 2 (standard error = 0.2) found here, suggests that in this set of experiments crystal growth might be controlled by surface incorporation, a result that is in accordance with an activation energy of 22.7 kcal/mol (standard error = 1.7) as pointed out by Shi et al.<sup>16</sup> A similar growth limitation mechanism was found in sucrose solution at low temperatures, below 40 °C.<sup>1</sup>

The effects of temperature and supersaturation on crystallisation rate can be also appreciated from Figure 7. Similar effects to those found when analysing bulk crystallisation (Figs. 3 and 4) are observed. The increase in growth rate with increasing supersaturation is accentuated when working at higher temperatures. This result is in agreement with those reported by Jelen and Coulter.<sup>25</sup> However, the dependence of growth rate on supersaturation and temperature found here may not be valid under other conditions (i.e., growth rate increases quad-

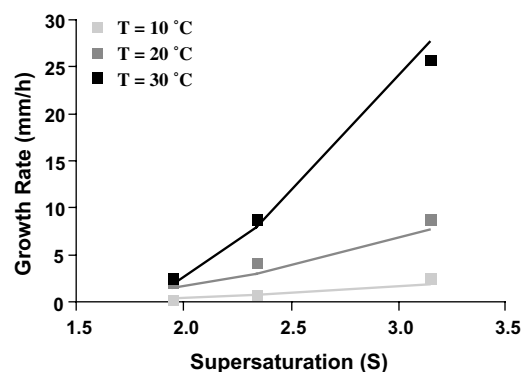


Figure 7. Experimental and predicted mean growth rates for different supersaturations and temperatures.

rationally with  $(S - 1)$  and exponentially with temperature), where mobility of the system may become relevant.

Deviations in the growth rate of digitally isolated single crystals were determined under all experimental conditions. This phenomenon known as growth rate dispersion (GRD) has been observed in many systems before.<sup>1</sup> GRD has been previously observed in secondary nucleation experiments and during the growth of crystal seeds at laboratory and industrial levels.<sup>1,16</sup> To date, no reports on GRD for spontaneous nucleation have been reported in the literature. As shown in Figures 8 and 9, from the data collected in this study it can be observed that higher temperatures and higher supersaturations induce wider rate dispersions. In other words, GRD becomes wider as the mean growth rate increases, as observed by Shi et al. for lactose secondary nucleation.<sup>16</sup> The influence of supersaturation on GRD is stronger than the influence of temperature (Fig. 9).

Additional experiments isolating faces (010) and (011) were carried out to investigate GRD phenomena when considering other faces. Results showed that

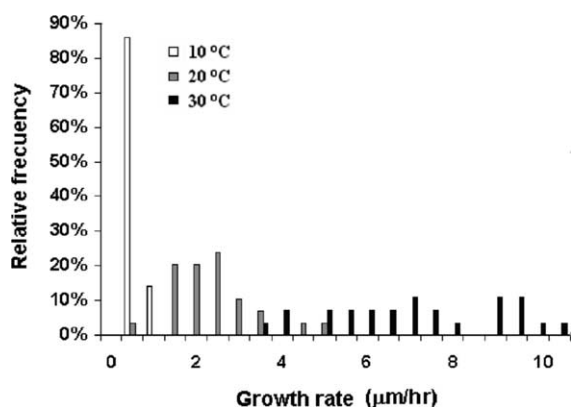


Figure 8. Growth rate dispersion for supersaturation of 1.95 at three different temperatures.

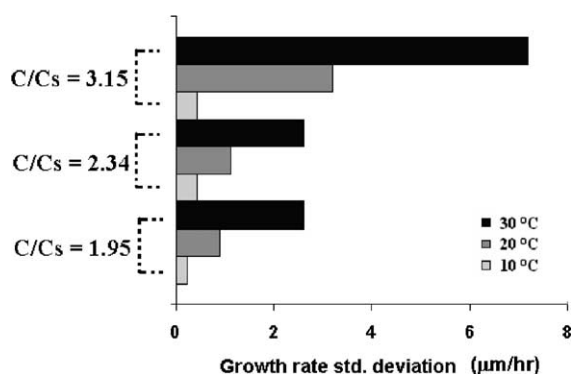


Figure 9. Standard deviation of the growth rates at different temperatures and supersaturations.

GRD was magnified when taking into account the growth rates of other crystal faces at the same experimental conditions.

Image analysis is an extremely powerful tool that allows not only the determination of crystallisation rates but also several shape parameters of interest. The ranges of selected geometrical dimensions that account for the crystal shape of the projected image of faces (110), (100) and (110) at the end of every experiment are presented in Table 2. Both parameters, aspect and roundness, tended to increase slowly at the beginning of the experiment, reaching a rather constant value over time. The subtle changes in shape that appear with increasing supersaturation could not be clearly identified using these shape parameters. For instance, the change from a triangular shape (supersaturations of 1.95 and 2.34; Fig. 6a) to a trapezoidal one (supersaturations of 3.15; Fig. 6b) could not be distinguished using these parameters. No clear pattern could be identified; however, the ranges for roundness and aspect tended to become shorter when temperature or supersaturation increased, suggesting that more homogenous-shaped crystals are obtained at higher temperatures and higher supersaturations. In addition, the values obtained for roundness and aspect are useful to discriminate lactose crystals from other crystals or, for instance, from lactose crystal agglomerates, which generally attain values of roundness greater than 2.

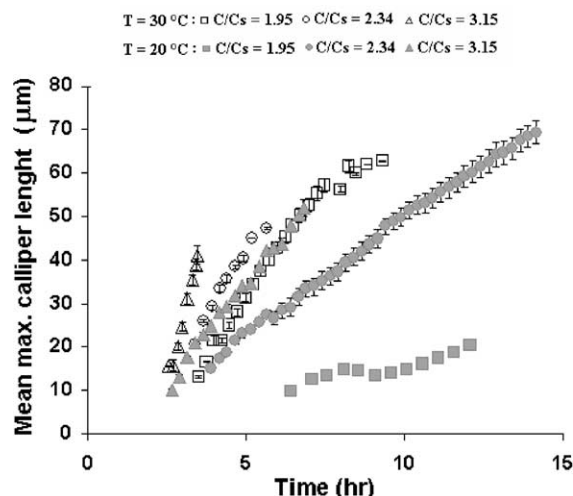
Another interesting feature of image analysis is its capacity to assess crystal size and eventually crystal size distribution during crystallisation from spontaneous nucleation. The particle size can be determined using different dimensions such as the calliper length, the mean diameter and the major axis of the equivalent ellipse, among others. The proper size will depend on the use given to the obtained data. For instance, if surface roughness of a product needs to be evaluated, the maximum calliper length of the crystal should be considered because it has been identified as the key dimension in surface roughness perception.<sup>29</sup> A graph showing

Table 2. Shape parameters ranges for single crystals at the end of every experiment

Relative supersaturation ( $C/C_s$ )	Temperature ( $^{\circ}\text{C}$ )	Aspect <sup>a</sup>	Roundness <sup>b</sup>
1.95	10	1.3–1.7	1.1–1.5
1.95	20	1.2–2.0	1.1–1.5
1.95	30	1.8–2.2	1.4–1.7
2.34	10	1.8–2.8	1.4–2.0
2.34	20	1.8–2.2	1.3–1.6
2.34	30	1.5–1.8	1.2–1.4
3.15	10	1.4–2.0	1.2–1.5
3.15	20	1.2–1.6	1.1–1.3
3.15	30	1.1–1.3	1.1–1.3

<sup>a</sup> Aspect is the ratio between the major axis and the minor axis of an equivalent ellipse.

<sup>b</sup> Roundness is defined as  $\text{perimeter}^2/4\pi\text{area}$ .



**Figure 10.** Mean maximum calliper length when crystallising at 20 and 30°C. Points are mean  $\pm$  standard error.

maximum calliper length of the same crystals that were studied to determine growth rates is shown in Figure 10. It can be seen that at early stages, larger crystals are observed at higher temperatures and at higher supersaturations.

In summary, a non-invasive method to follow spontaneous lactose crystallisation based on microphotograph acquisition in situ (hot-stage microscopy) was successfully implemented. The technique proved to be instrumental in early stages of crystallisation when the system was defined by a two dimensional crystal growth front, allowing visualisation and quantification of changes in real time. It is believed that a similar experimental set-up could be implemented in a real food system to miniaturise a particular process where crystallisation control is of interest and where traditional techniques are difficult to implement. In this way not only could crystallisation kinetics be followed, but also other parameters accounting for the crystal shape could be successfully derived by means of image analysis. This information could be used selectively to study the influence of key geometrical features on sensory perception or on macroscopic properties of interest such as texture.

### 3. Experimental

#### 3.1. Preparation of solutions

Supersaturated solutions were prepared by heating at  $70 \pm 2^\circ\text{C}$  a specific amount of  $\alpha$ -lactose monohydrate (edible grade, Michelson, Santiago, Chile) in distilled water using a stirring hot plate (Thermolyne, Dubuque, USA), until all lactose entered solution. The solution under study was then stored for 2 h at the selected crys-

tallisation temperature  $\pm 0.5^\circ\text{C}$  in a forced air oven (Memmert, Schwabach, Germany) to allow for thermal stabilisation. Subsequently, 0.4 mL of the solution under study were poured into a circular glass holder (diameter = 18 mm, height = 8 mm), covered with a glass slip and sealed with silicone to avoid water evaporation.

Three crystallisation temperatures (10, 20 and  $30^\circ\text{C}$ ) and three different levels of initial relative supersaturation ( $C/C_s = 1.95$ ; 2.34; 3.15, where  $C$  stands for lactose concentration and  $C_s$  stands for lactose solubility at the specific temperature) were investigated. Because lactose solubility data available in the literature show some variation depending on the source, a solubility curve was obtained by calculating mean solubility values from two different sources.<sup>30,31</sup>

#### 3.2. Hot-stage experiments

The glass holder containing the solution was placed on a hot stage (model THMS 600, Linkham Scientific, Surrey, UK) set at the corresponding temperature  $\pm 0.1^\circ\text{C}$ , adapted to an Olympus BX 50 polarised light microscope (Olympus Optical Corporation, Tokyo, Japan) and viewed with a  $4\times$  magnifying lens, as shown in Figure 11. Images were acquired with a CoolSnap Pro digital camera (Media Cybernetics, Silver Spring, USA), providing an extra  $10\times$  magnification, giving an overall magnification of  $40\times$ .

Images were continuously acquired at time intervals ranging from 3 to 60 min depending on the experiment. Each experiment was ended when crystals started to overlap, generating a three dimensional crystallisation front. Subsequently, the recorded images were processed and analysed using Image Pro Plus 4.5 software (Media Cybernetics, Silver Spring, USA).

The resulting microphotographs were not in the optimum condition for immediate image analysis and conse-

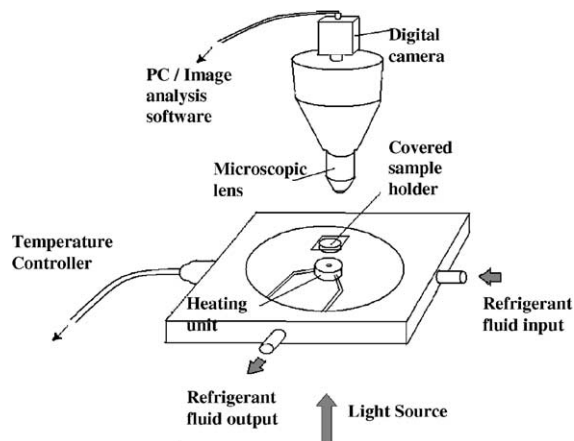


**Figure 11.** Schematic diagram of the digital imaging system used to assess lactose crystallisation.



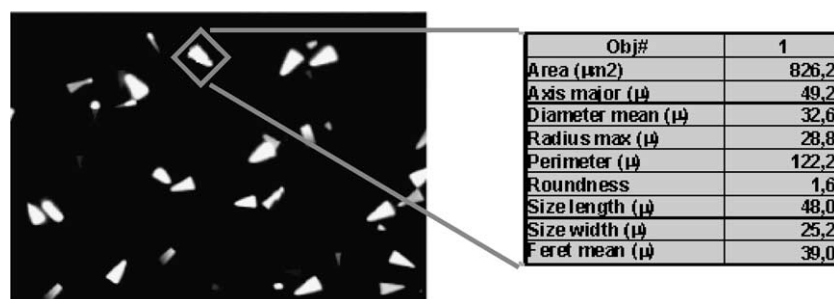


**Figure 12.** Digital isolation of a single crystal showing some of the geometrical parameters that can be quantified. This image is from an experiment carried out at  $C/C_s = 1.95$  and  $30^\circ\text{C}$ .

quently, an image processing protocol was established. The developed procedure aimed to homogenise the background of the image and to increase the number of crystals that could be recognised as objects by the software. First, the background of the image was extracted using a background extracting filter, which was then subtracted from the original image to attain a homogeneous background. Thereafter, the image was converted into an eight-bit grey scale image and the associated grey-level histogram was generated. Large differences in grey level between lactose crystals and the background were found in all experiments. The obtained bimodal histogram allowed easy segmentation of lactose crystals from the background by thresholding. That is, grey levels that fell below an intensity limit (threshold) were arbitrarily set to equal 0 (black) and all other values set to 255 (white). Selection of the proper threshold was carried out by trial and error, guided by visual observation of the result. Setting a fixed grey level value of 74 as threshold assured an appropriate recognition of crystals including their dimmest regions for all experiments. Finally, a binary representation of the image was obtained with only two intensity values, 0 and 255, allowing the different objects to be clearly distinguished.

To characterise lactose crystallisation kinetics, two analyses were performed in every image sequence. The first analysis consisted of determining the total area occupied by crystals in a microscopic field ( $1.2 \times 1.6\text{mm}$ ) for increasing crystallisation times, to derive bulk crystallisation kinetics. The second analysis consisted of the digital isolation and quantitative characterisation of single crystals to determine geometrical parameters of interest, such as perimeter, diameter, area, roundness and Feret mean and to derive crystal growth rates (see Fig. 12).

All experiments were carried out in triplicate for each experimental condition. Furthermore, to characterise single crystals, approximately nine crystals were isolated in each experiment, ensuring that all selected individual crystals were completely separated from their neighbours during the whole experiment.

### 3.3. Refractometric measurements

Additionally, lactose crystallisation was followed using an Abbe 3T refractometer (with an accuracy of  $\pm 0.0002$ , Atago, Tokyo, Japan) at  $25^\circ\text{C}$ , under the same experimental conditions. This corresponds to an indirect measure of crystallisation, which is carried out by evaluating the change in solution characteristics (de-supersaturation). The crystallisation temperature was maintained by storing the glass holder with the solution in the same forced air oven. When working with supersaturations of 2.34 and 3.15 the solution was sampled every hour during the first 10 h and subsequently after 24, 48, 72 and 96 h. When working with a supersaturation of 1.95 the solution was sampled every 2 h during the first 10 h and subsequently after 24, 48, 72 and 96 h. To do this, 0.15 mL were extracted from the solution under study, which were then poured into a sedimentation tube and were allowed to settle for 15 min. Finally, 0.03 mL were extracted from the sedimentation tube and the refractive index (RI) was measured. Solutions of different concentrations of lactose in water were prepared and a plot of lactose concentration against RI over the whole concentration range of interest was obtained. This calibration curve was used to derive the mass of crystallised lactose for increasing times at each experimental condition. Every experiment was carried out in triplicate.

Statistical analysis of results was carried out using Statgraphics Plus 4.0 (Statistical Graphics Corp., Maryland, USA).

### Acknowledgements

Financial support from Fondecyt project 1020796 is highly appreciated.

### References

1. Hartel, R. W. Crystal Growth. In *Crystallization in Foods*; Aspen Publishers: Gaithersburg, 2001; pp 192–211.

2. Belitz, H. D.; Grosh, W. Milk and Dairy Products. In *Food Chemistry*, 2nd ed.; Guna, S., Springer: Berlin, 1999; pp 470–512.
3. Raghavan, S. L.; Ristic, R. I.; Sheen, D. B.; Sherwood, J. N.; Trowbridge, L.; York, P. J. *Phys. Chem. B* **2000**, *104*, 12256–12262.
4. Haase, G.; Nickerson, T. A. *J. Dairy Sci.* **1966**, *49*, 757–761.
5. Twieg, W. C.; Nickerson, T. A. *J. Dairy Sci.* **1968**, *51*, 1720–1724.
6. Valle-Vega, P.; Nickerson, T. A. *J. Food Sci.* **1977**, *42*, 1069–1072.
7. Nickerson, T. A.; Moore, E. E. *J. Dairy Sci.* **1973**, *57*, 160–164.
8. Nickerson, T. A.; Moore, E. E. *J. Dairy Sci.* **1974**, *57*, 1315–1319.
9. Hartel, R. W.; Shastry, A. V. *Crit. Rev. Food Sci. Nutr.* **1991**, *1*, 49–112.
10. Stanley, D. W.; Aguilera, J. M.; Baker, K. W.; Jackman, R. L. Structure/Property Relationships of Foods as Affected by Processing and Storage. In *Phase/State Transitions in Foods*; Rao, M. A., Hartel, R. W., Eds.; Marcel Dekker: New York, 1998; pp 1–56.
11. Aguilera, J. M.; Stanley, D. W. Examining Microstructure. In *Microstructural Principles of Food Processing and Engineering*, 2nd ed.; Aspen Publishers: Gaithersburg, 1999; pp 1–70.
12. Van Kreveland, A.; Michaels, A. S. *J. Dairy Sci.* **1965**, *48*, 259–265.
13. Kucharenko, J. A. *Planter Sugar Manuf.* **1928**, *81*, 2.
14. Aguilera, J. M.; Lillford, P. J. Microscopy and Image Analysis as Related to Food Engineering. In *Food Engineering 2000*; Fito, P., Ed.; Chapman & Hall: London, 1996; pp 23–38.
15. Bouchon, P.; Aguilera, J. M. *Int. J. Food Sci. Technol.* **2001**, *36*, 669–676.
16. Shi, Y.; Hartel, R. W.; Liang, B. *J. Dairy Sci.* **1989**, *72*, 2906–2915.
17. Visser, R. A. *Neth. Milk Dairy J.* **1982**, *36*, 167–193.
18. Liang, B. M.; Hartel, R. W.; Berglund, K. A. *AIChE J.* **1987**, *33*, 2077–2079.
19. Aguilera, J. M. *Food Sci. Technol. Int.* **2003**, *9*, 137–143.
20. Aguilera, J. M.; Baffico, P. *J. Food Sci.* **1997**, *62*, 1048–1053, 1066.
21. Aguilera, J. M.; Cadoche, L.; Lopez, C.; Gutierrez, G. *Food Res. Int.* **2001**, *34*, 939–947.
22. Mazzobre, M.; Aguilera, J. M.; Buera, P. *Carbohydr. Res.* **2003**, *338*, 541–548.
23. Howell, T.; Hartel, R. *J. Food Sci.* **2001**, *66*, 979–984.
24. Shanks, B. H.; Berglund, K. A. *AIChE J.* **1985**, *31*, 152–154.
25. Jelen, P.; Coulter, S. T. *J. Food Sci.* **1973**, *38*, 1128–1185.
26. Thurlby, J. A. *J. Food Sci.* **1976**, *41*, 38–42.
27. Garnier, S.; Petit, S.; Coquerel, G. *J. Cryst. Growth* **2002**, *234*, 207–219.
28. Bhargava, A.; Jelen, P. *J. Food Sci.* **1996**, *61*, 180–184.
29. Hough, G.; Martinez, E.; Contarini, A. *J. Dairy Sci.* **1990**, *73*, 604–611.
30. Nickerson, T. A. Lactose. In *Fundamentals of Dairy Chemistry*; Webb, B. H., Johnson, A. H., Alford, J. A., Eds.; AVI Publishers: Westport, 1974; pp 356–380.
31. Ullmann, F. Lactose and Derivatives. In *Ullmann's Encyclopedia of Industrial Chemistry*; Gerhartz, W., Ed.; VCH: Florida, 1985; pp 107–113.